FEBS Letters 524 (2002) 92–96 FEBS 26299

# Polyene antibiotic amphotericin B in monomolecular layers: spectrophotometric and scanning force microscopic analysis

Wieslaw I. Gruszecki[a,*], Mariusz Gagos[a,b], Peter Kernen[c,1]

[a] *Department of Biophysics, Institute of Physics, Maria Curie-Sklodowska University, 20-031 Lublin, Poland*
[b] *Department of Physics, Agricultural University, Lublin, Poland*
[c] *EMPA, Swiss Federal Laboratories for Materials Testing and Research, Lerchenfeldstrasse 5, 9014 St. Gallen, Switzerland*

Received 10 April 2002; revised 18 June 2002; accepted 19 June 2002

First published online 8 July 2002

Edited by Maurice Montal

**Abstract Monolayers of amphotericin B (AmB) and monolayers composed of AmB and dipalmitoylphosphatidylcholine (DPPC) were formed at the argon–water interface and deposited on a solid support by means of the Langmuir–Blodgett technique. The hypsochromic shift observed in the absorption spectra of monolayers is indicative of aggregated structures of AmB. The exciton splitting theory allowed us to calculate the distance between neighboring molecules in the aggregates as 7.8 Å. Scanning force microscopy of the AmB monolayers revealed the formation of a homogeneous monolayer composed of molecules separated by a distance of 6–8 Å. Microscopy also reveals the formation of cylindrical structures of AmB with a diameter close to 17 Å (internal diameter close to 6 Å) in the monolayers containing additionally 10 mol% DPPC.** 

*Key words:* Amphotericin B; Exciton splitting; Monolayer; Membrane pore; Polyene antibiotic; Atomic force microscopy

## 1. Introduction

Amphotericin B (AmB) is a popular polyene antibiotic widely used to treat deep-seated mycotic infections [1,2]. According to the current opinion the main mode of action of AmB is based on the formation of hydrophilic molecular pores in a membrane environment [3,4]. For the particular ability to form membrane pores in the presence of ergosterol, the fungal sterol, there are two main modes of action of AmB, both based on the formation of pores across a biomembrane: molecular pores formed solely by the drug [3,4] and pores formed as two-component molecular structures of AmB and sterols, in particular ergosterol [5,6]. The ability of AmB to form cylindrical molecular aggregates follows directly from its very specific stereochemical structure (see inset in Fig. 1). AmB is an amphiphilic molecule with several polar groups located along one side of the molecule. Polar groups are preferentially exposed outside in a polar environment and covered inside molecular assemblies formed in a hydrophobic environment in order to minimize the energy [7] of the system. Self-organization of AmB in a polar and hydrophobic environment was the subject of numerous recent theoretical and experimental studies [8–11]. In particular the organization of AmB in the environment of lipid membranes has been recently addressed as directly relevant to the pharmacological usefulness of the drug [12–15]. There are several lines of support for the concept of formation of membrane channels by AmB, mainly based on the results of experiments with ion permeability across lipid membranes [4,16–18]. In this report we present for the first time a direct indication of the size of such a molecular pore formed by AmB based on pronounced spectral shifts of electronic absorption bands of substrate-supported AmB monolayers and scanning force microscopy imaging of the surface topography of monomolecular layer composed of the drug and dipalmitoylphosphatidylcholine (DPPC).

## 2. Materials and methods

AmB in crystalline form and DPPC were purchased from Sigma. AmB was dissolved in 40% 2-propanol and then centrifuged for 15 min at $15\,000\times g$ in order to remove microcrystals of the drug still remaining in the sample. AmB was further purified by means of HPLC on a YMC C-30 coated reversed phase column (length 250 mm, internal diameter 4.6 mm) with 40% 2-propanol in $H_2O$ as the mobile phase. The final concentration of AmB was calculated from the absorption spectra on the basis of the molar extinction coefficient to be $1.3\times10^5$ $M^{-1}$ $cm^{-1}$ in the 0-0 absorption maximum at 408 nm. DPPC was dissolved in chloroform. Monomolecular layers of the AmB–DPPC system were formed at the argon–water interface by a method described in detail previously [15]. As a first step DPPC was deposited at the interface and after 15 min, required for solvent evaporation, AmB solution was deposited at many places of the interface. Monolayers were formed on double distilled and deionized water distilled for a third time with $KMnO_4$ in order to remove possible organic impurities. Monomolecular layers were formed in a Teflon trough 40 cm × 4 cm and were compressed along the long side with a speed of 4.8 $cm^2$/min. Surface pressure was monitored by a NIMA Technology tensiometer, model PS3 (Coventry, UK). Monolayer compression, surface pressure measurements and data acquisition were controlled by our own software. Langmuir–Blodgett films were deposited on quartz, for optical measurements, and on mica for scanning force microscopic measurements with a speed of 0.5 cm/min at a constant surface pressure of 30 mN/m, using a Lauda Filmlift, model FL-1E (Lauda, Königshafen, Germany). Monolayer compression and deposition was carried out at 23 ± 1°C. In order to avoid oxidative degradation of a monolayer during compression experiments were performed in darkness under argon atmosphere. Electronic absorption spectra were recorded with a Shimadzu 160A UV-Vis spectrophotometer. Spectra were analyzed with Grams 32 software from Galactic Industries. Scanning force microscopy (SFM) was carried out with dry samples in air on a NanoScope III (Digital Instruments, Santa Barbara, CA, USA) with scan speeds around 1 Hz. Microfabricated monocrystalline silicon tips with force constants ranging from 0.06

*Corresponding author. Fax: (48)-81-537 61 91.
*E-mail address:* wieslaw@tytan.umcs.lublin.pl (W.I. Gruszecki).

[1] Present address: Zyomyx, Inc., 26101 Research Road, Hayward, CA 94545, USA.

0014-5793/02/$22.00 
PII: S0014-5793(02)03009-0

to 0.17 N/m were used for contact mode imaging (from LOT, Darmstadt, Germany). All SFM images are raw data except corrected for image levelling.

## 3. Results and discussion

Fig. 1 presents isotherms of compression of the single monomolecular layers formed at the argon–water interface with pure AmB and a two-component system composed of 90 mol% AmB and 10 mol% DPPC. The shape of the isotherm of compression of AmB is very close to the shape of isotherms previously reported [15,19–22]. The compression of AmB is a two-phase process represented by two distinct linear portions of the isotherm of compression pointing to the specific molecular areas of 136 Å$^2$ and 36 Å$^2$. These specific areas correspond to different molecular arrangements of AmB at the argon–water interface, most probably the horizontal one (AmB anchored in the subphase with polar groups located along its longer axis) at low surface pressure values and the vertical one (AmB anchored in the subphase with its sugar binding side (see inset of Fig. 1) [15]. The specific area of 36 Å$^2$ is close to the theoretical cross-section of AmB which can be calculated on the basis of crystallographic parameters (approximately 6 Å×7 Å [3]), which is an indication of very efficient packing of AmB in the monomolecular layer despite the amphiphilic character of this molecule. Most probably the arrangement of AmB in a monolayer is such that polar groups of neighboring molecules interact with each other in order to minimize the energy of the system, such as in the case of dimer formation [9]. The relatively high collapse pressure values of AmB monolayer (above 32 mN m$^{-1}$) is an indication that such structures are potentially stable also in lipid biomembranes characterized typically by the surface pressures close to 30 mN m$^{-1}$ [23]. The distinct plateau phase in the molecular area range of 100 Å$^2$ to 40 Å$^2$ corresponds to the reorientation of AmB at the interface, in light of recent Brewster angle microscopic analysis of monomolecular layers of AmB [22]. Such a clear transition phase has not been observed in our previous experiments [15], in the same system compressed with higher speed (30 cm$^2$/min versus 4.8 cm$^2$/min in the present work). Relatively slow compression provided quasi-static conditions, which are most probably responsible for reorientation of AmB molecules at virtually constant surface pressure close to 10 mN m$^{-1}$. On the other hand, the speed of compression had no effect on the value of the specific molecular areas corresponding to two orientations of AmB at the interface. Fig. 1 also presents the isotherm of compression of the two-component monomolecular layer formed with AmB and DPPC. The presence of the lipid component in the AmB layer (10 mol% DPPC) has an effect in the slight decrease in the specific molecular areas corresponding to both molecular arrangements of AmB at the interface (by ca. 3 Å$^2$). The specific molecular area of DPPC under the same conditions is close to 59 Å$^2$ [15] and therefore the decrease in two specific molecular areas of AmB (corresponding to both orientations at the interface) is an indication of modified packing of the drug in the presence of a lipid component. Molecular packing in the AmB–DPPC films can be analyzed in terms of the additivity rule. In the case of a vertical arrangement of AmB the dependence for the mean molecular area has the form:

$$0.90\times 36\ \text{Å}^2 + 0.10\times 59\ \text{Å}^2 = 38.3\ \text{Å}^2 \quad (1)$$

As may be seen the theoretical value of the average molecular area is slightly greater than the experimental one, 34 Å$^2$. This is an indication of the ordering effect of the lipid component with respect to the AmB molecules in a monolayer. No strong over-additivity was observed in the present experiments, upon very slow compression of a monolayer. Such a

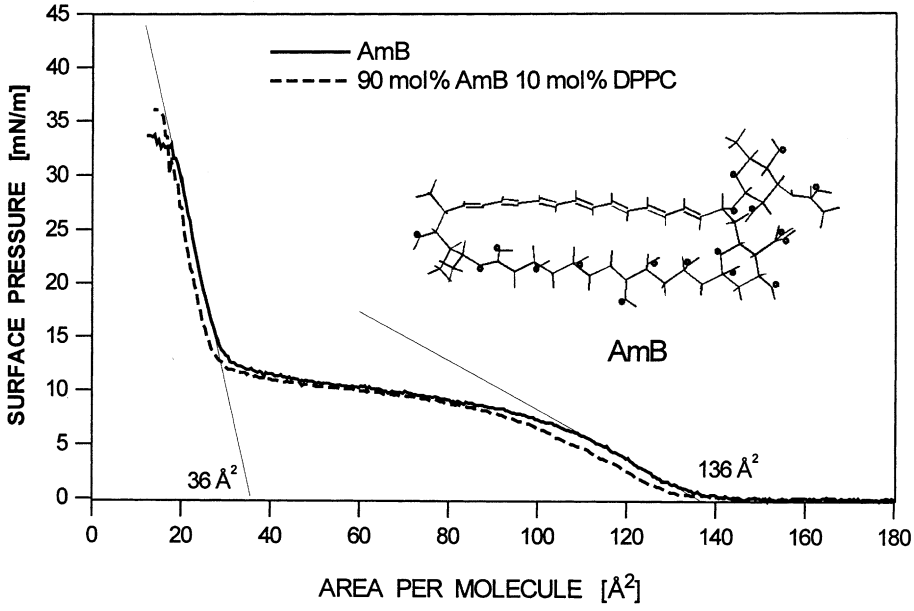


Fig. 1. Isotherms of compression of monomolecular layers formed with pure AmB (solid line) and 90 mol%/10 mol% DPPC (dotted line). The linear fits to the linear portions of the isotherms of compression extrapolated to zero surface pressure point to the specific molecular areas. Inset, chemical structure of AmB generated by the HyperChem software from Hypercube Inc., based on the crystallographic data from [3] (polar oxygen groups marked with rings).

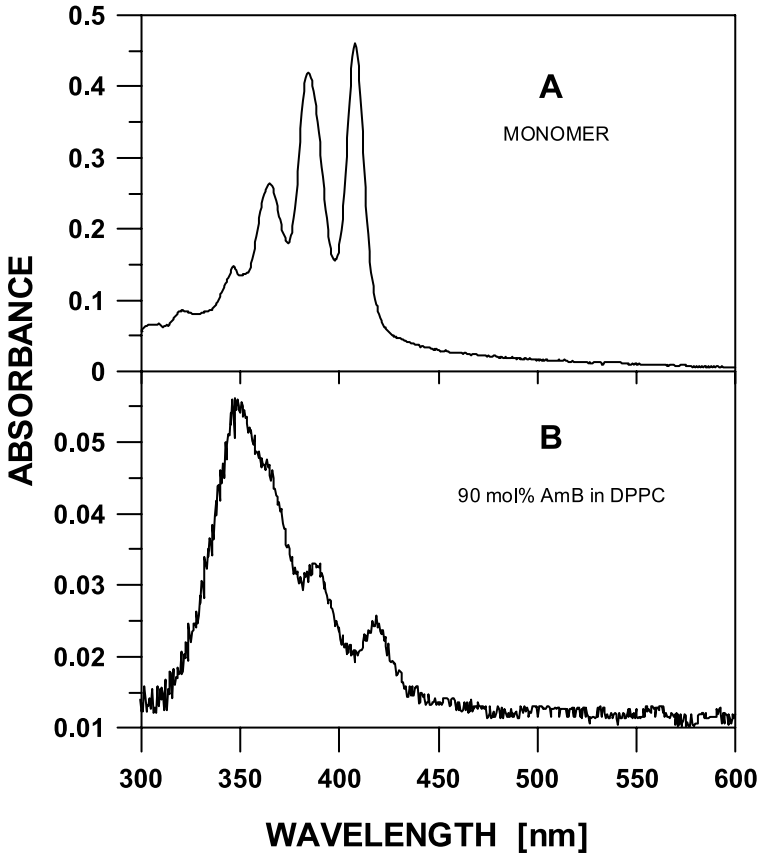


Fig. 2. Electronic absorption spectra of AmB in monomeric form in solution (water:2-propanol 3:2, v/v) and recorded from Langmuir–Blodgett monomolecular films deposited at two sides of a quartz lamella from the two-component monomolecular film formed with 90 mol% AmB and 10 mol% DPPC. The Langmuir–Blodgett film was tilted by 45° with respect to the measuring beam.

result is an indication of very efficient molecular packing within a monolayer characterized by small intermolecular distances.

A small distance between chromophores of the neighboring AmB molecules shell results in affection of the singlet excitation energy levels, which can be potentially observed in electronic absorption spectroscopy. Fig. 2 presents absorption spectra of AmB in monomeric form in the deposition solution and in monomolecular layer deposited on a quartz slide as a Langmuir–Blodgett film. A very clear and large hypsochromic shift can be observed in the AmB spectrum in monolayer in accordance with the expectation based on analysis of the isotherms of compression. The absorption spectrum of AmB dissolved in 40% 2-propanol displays the typical shape characteristic of a monomeric form of AmB with the 0-0 vibronic transition localized at 408 nm [7]. A pronounced hypsochromic shift combined with the loss of a clear vibronic structure is an indication of the formation of H-type aggregated molecular structures [11,24,25]. The spectral shift of the 0-0 vibronic transition, also visible in the spectrum of AmB in monolayers at 418 nm (23 923 $cm^{-1}$), to the main absorption band corresponding to the aggregated form, 348 nm (28 736 $cm^{-1}$), is 4813 $cm^{-1}$. The exciton splitting theory directly links a spectral shift to spectral parameters of a chromophore and the number of molecules involved in a formation of such an aggregated structure [25]:

$$\nu_m = \nu_{\mathrm{mon}} + 2\beta\cos\left(\frac{m\pi}{N+1}\right) \tag{2}$$

where $\nu_m$ is the position of the $m$-th excitation state in the spectrum of the aggregated form, $\nu_{\mathrm{mon}}$ is the position of the electronic transition in the spectrum of monomeric chromophores, $N$ is the number of all exciton states and $m$ is the number of the exciton state considered. In the case of maximum hypsochromic shift $m=1$. The parameter $\beta$ represents the coupling matrix element and has the form [25]:

$$\beta = \frac{|\mu_{\mathrm{mon}}|^2}{4\pi\varepsilon_0\eta^2R^3}(\cos\theta - 3\cos^2\phi) \tag{3}$$

where $\mu_{\mathrm{mon}}$ is the dipole transition moment of a monomer, $\varepsilon_0$ is the dielectric permittivity of free space, $\eta$ is the refractive index of the medium and $R$ is the distance between nearest neighbors in the aggregate. The angle between monomeric transition moment vector $\theta$ and the angle between the transition moment vector and the axis connecting the centers of the transition moment vectors of neighbor molecules $\phi$ were assumed to be 0° and 90° in the case of H-aggregates of AmB in compressed monolayers respectively [11]. A value of 11.3 Debye for the transition dipole of monomeric AmB was calculated based on the integration of the absorption spectra. The hypsochromic shift accompanying AmB aggregation in monomolecular layers, 4813 $cm^{-1}$ ($\nu_{\mathrm{m}} - \nu_{\mathrm{mon}}$), and the value of $\mu_{\mathrm{mon}}$ enabled calculation of the molecular distance between the neighbor AmB molecules in the aggregated structure assuming a high number of molecules involved ($\nu_{\mathrm{m}} - \nu_{\mathrm{mon}} = 2\beta$) as $R = 7.8$ Å.

Monomolecular layers formed with AmB and two-compo-

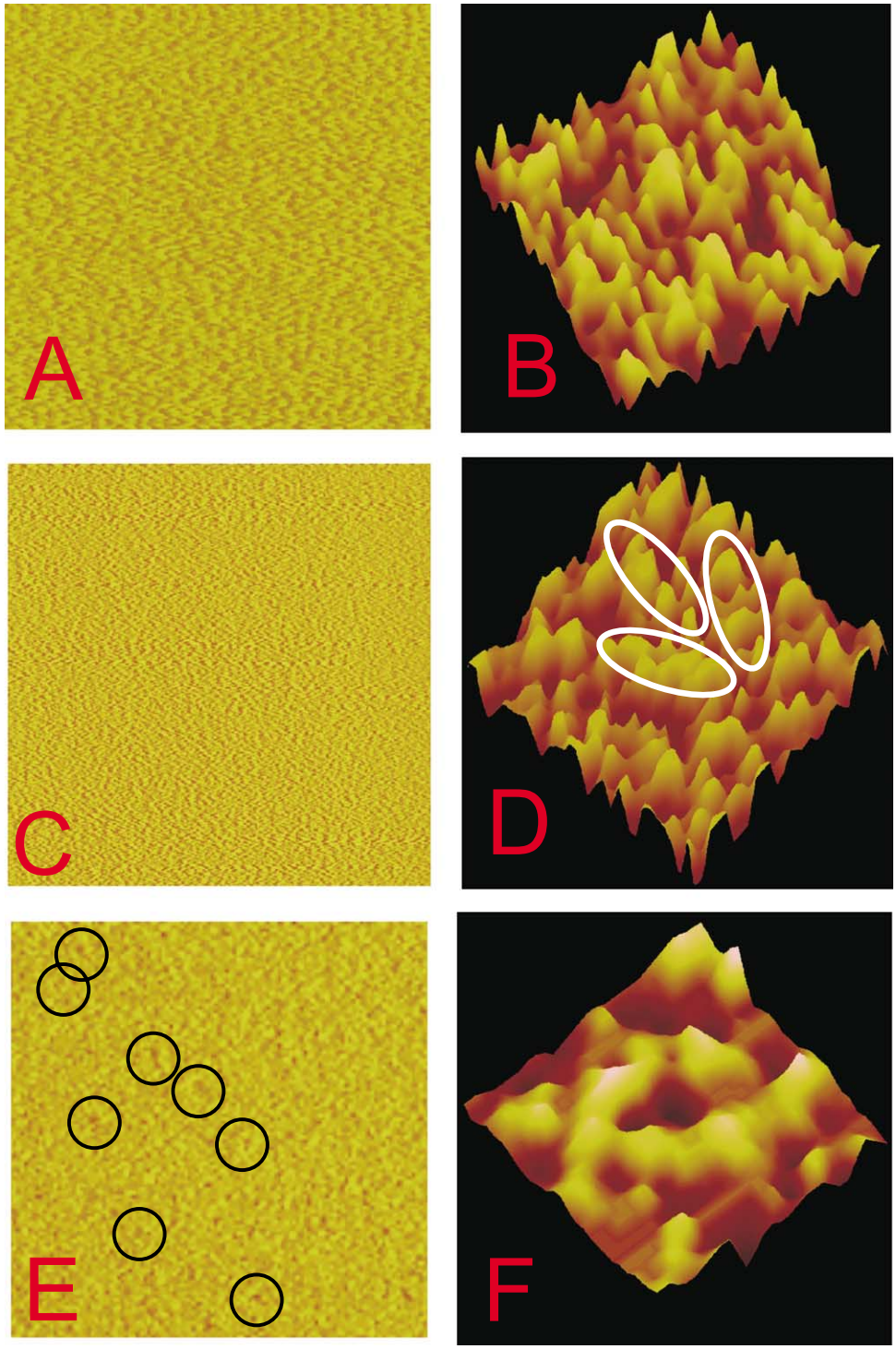


Fig. 3. SFM images recorded in deflection mode of mica (A,B), monocomponent AmB monolayer deposited to mica (C,D) and two-component AmB–DPPC monolayer (9:1) deposited on mica (E,F). The scan sizes for A, C and E are 20 nm×20 nm with a $z$ range of 0.1 nm. The 3D views (B, D and F) are shown with scan sizes of 2 nm×2 nm (B,F) and 1.7 nm×1.7 nm (D). All 3D images shown here are plotted with a $z$ range of 0.1 nm. The molecular structures interpreted as single AmB molecules in D are marked with white ellipses and the selected pore-like structures in E by black circles.

nent monomolecular layers formed with AmB and DPPC were also deposited on mica and the topography of the film surface was imaged with SFM. Fig. 3 presents the SFM images of deposited monolayers and the surface topography of mica alone as a control. In general, the surfaces of both monolayers deposited on mica are less rough than the support itself, as may be seen from Fig. 3. This effect, related to the relatively high lateral pressure of compact monolayers, has also been observed in the case of other supports [26]. As can be seen from Fig. 3C, the molecular arrangement in the pure AmB monolayer is very much homogeneous. The shapes (marked with white ellipses) corresponding to single AmB

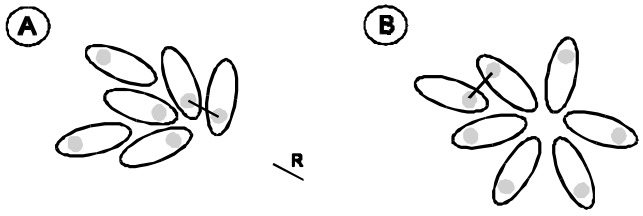


Fig. 4. Schematic representation of a molecular arrangement of AmB in monomolecular film. (A) Semi-homogeneous distribution. (B) Formation of ring-like structures. Molecules are represented by ellipses and chromophores by gray circles. *R* denotes distance of neighboring chromophores.

molecules can be noticed in the small size scan of this monolayer (Fig. 3D) but the level of noise makes such an assignment practically at the limit of significance. Fig. 3E presents a 20-nm image of the topography of the AmB monolayer containing 10 mol% DPPC as a second component. The molecular arrangement in such a monolayer is different, according to the analysis of surface pressure–molecular area isotherms of compression. The small under-additivity effect observed is an indication of molecular interaction between components and most probably an ordering effect of DPPC with respect to AmB, owing to the low concentration of the lipid component. This effect is most probably associated with the presence of hydrophobic alkyl chains of DPPC in the system composed of molecules that are amphiphilic in the plane of a layer, such as AmB. Also the surface topography of the two-component monolayer (Fig. 3E) is different from the topography of the monolayer formed with pure AmB. The pore-like structures can be observed in the two-component monolayers, which do not correspond to any features in the pure AmB Langmuir–Blodgett films and the control. Some of these structures are marked with circles in Fig. 3E and one pore is presented on a 2-nm scale (Fig. 3F). The external diameter of the pore-like structures was determined as close to $17 \pm 3$ Å and the internal diameter as close to $6 \pm 1$ Å on the basis of surface cross-section analysis (average from eight structures ±S.D.). The diameter of the rings observed implies that the structure is formed by six to eight AmB molecules according to the analysis procedure described previously [11]. Fig. 4 presents a simplified model of arrangement of AmB molecules in the monomolecular layers based on both spectroscopic measurements and SFM imaging. The distance *R* between the neighboring AmB molecules calculated above as 7.8 Å, on the basis of the exciton splitting theory, corresponds well to the distance that may be deduced from the atomic force microscopy (AFM) images, between 6 Å and 8 Å (Fig. 3D). To our knowledge our report also presents the first direct visualization of AmB pores that are potentially active pharmacologically. The external diameter of the ring-like structures of AmB observed (17 Å) implies that the internal diameter of a hydrophilic pore of such a structure is about 5 Å, taking into account the dimensions of an AmB molecule in the monolayers (specific molecular area 36 $Å^2$, corresponding to the linear dimension of 6 Å). This estimation of the diameter of the hydrophobic pore corresponds to the cross-section analysis of the AFM images ($6 \pm 1$ Å). These results indicate that the AmB pore is rather not specific for small ions and may influence considerably membrane transport properties for water and also small molecules. It is possible that interactions of AmB to sterols may further increase the radius of the pore.

*Acknowledgements:* The authors would like to thank Michael Sondergaard for his cooperation at the early stage of this research. The State Committee of Scientific Research of Poland is acknowledged for financial support within Project 3P04A 076 22.

## References

[1] Janoff, A.S., Boni, L.T., Popescu, M.C., Minchey, S.R., Cullis, P.R., Madden, T.D., Taraschi, T., Gruner, S.M., Shyamsunder, E., Tate, M.W., Mendelsohn, R. and Bonner, D. (1988) Proc. Natl. Acad. Sci. USA 85, 6122–6126.
[2] Brajtburg, J., Powderly, W.G., Kobayashi, G.S. and Medoff, G. (1990) Antimicrob. Agents Chemother. 34, 183–188.
[3] Bonilla-Marin, M., Moreno-Bello, M. and Ortega-Blake, I. (1991) Biochim. Biophys. Acta 1061, 65–77.
[4] Fujii, G., Chang, J.-E., Coley, T. and Steere, B. (1997) Biochemistry 36, 4959–4968.
[5] DeKruijff, B., Gerristen, W.J., Oerlemans, A., Demel, R.A. and Van Deenen, L.L.M. (1974) Biochim. Biophys. Acta 339, 44–56.
[6] Cotero, B.V., Rebolledo-Antúnez, S. and Ortega-Blake, I. (1998) Biochim. Biophys. Acta 1375, 43–51.
[7] Bagiński, M., Gariboldi, P., Bruni, P. and Borowski, E. (1997) Biophys. Chem. 65, 91–100.
[8] Barwicz, J., Gruszecki, W.I. and Gruda, I. (1993) J. Colloid Interface Sci. 158, 71–76.
[9] Mazerski, J. and Borowski, E. (1996) Biochim. Biophys. Acta 57, 205–217.
[10] Caillet, J., Bergès, J. and Langlet, J. (1995) Biochim. Biophys. Acta 1240, 179–195.
[11] Gagoś, M., Koper, R. and Gruszecki, W.I. (2001) Biochim. Biophys. Acta 1511, 90–98.
[12] Tancrède, P., Barwicz, J., Jutras, S. and Gruda, I. (1990) Biochim. Biophys. Acta 1030, 289–295.
[13] Hamilton, K.S., Barber, K.R., Davis, J.H., Neil, K. and Grant, Ch.W.M. (1991) Biochim. Biophys. Acta 1062, 220–226.
[14] Fournier, I., Barwicz, J. and Tancrède, P. (1998) Biochim. Biophys. Acta 1373, 76–86.
[15] Wójtowicz, K., Gruszecki, W.I., Walicka, M. and Barwicz, J. (1998) Biochim. Biophys. Acta 1373, 220–226.
[16] Lambing, H.E., Wolf, B.D. and Hartsel, S.C. (1993) Biochim. Biophys. Acta 1152, 185–188.
[17] Vertut-Croquin, A., Bolard, J., Chabbert, M. and Gary-Bobo, C.M. (1983) Biochemistry 22, 2939–2944.
[18] Aracava, Y., Schreier, S., Phadke, R., Deslauriers, R. and Smith, I.C.P. (1981) Biophys. Chem. 14, 325–332.
[19] Saint-Pierre-Chazalet, M., Thomas, C., Dupeyarat, M. and Gary-Bobo, C.M. (1988) Biochim. Biophys. Acta 944, 477–486.
[20] Lance, M.R., Washington, C. and Davis, S.S. (1996) Pharm. Res. 13, 1008–1014.
[21] Seoane, R., Miñones, J., Conde, O., Casas, M. and Iribarnegaray, E. (1998) Biochim. Biophys. Acta 1375, 73–83.
[22] Miñones Jr., J., Carrera, C., Dynarowicz-Łątka, P., Miñones, J., Conde, O., Seoane, R. and Rodriguez Patino, J.M. (2001) Langmuir 17, 1477–1482.
[23] Gennis, R.B. (1988) Biomembranes. Molecular Structure and Function, Springer-Verlag, New York.
[24] Kasha, M. (1963) Radiat. Res. 20, 55–71.
[25] Parkash, J., Robblee, J.H., Agnew, J., Gibbs, E., Collings, P., Pasternack, R.F. and de Paula, J.C. (1998) Biophys. J. 74, 2089–2099.
[26] Kernen, P., Gruszecki, W.I., Matuła, M., Wagner, P., Ziegler, U. and Krupa, Z. (1998) Biochim. Biophys. Acta 1373, 289–298.